TITLE:

Exacerbated ozone pollution in the greening northern China

AUTHOR LIST:

1. Jiawei Xu (xujw@smail.nju.edu.cn); School of Atmospheric Sciences, Nanjing University; Collaborative Innovation Center for Climate Change, Jiangsu Province, Nanjing, China
2. Sijia Lou (lousijia@nju.edu.cn); School of Atmospheric Sciences, Nanjing University; Collaborative Innovation Center for Climate Change, Jiangsu Province; Frontiers Science Center for Critical Earth Material Cycling, Nanjing University, Nanjing, China
3. Nan Wang (nan.wang@smail.nju.edu.cn); School of Atmospheric Sciences, Nanjing University; Collaborative Innovation Center for Climate Change, Jiangsu Province, Nanjing, China
4. Lian Xue (lian.xue@nju.edu.cn); School of Atmospheric Sciences, Nanjing University; Collaborative Innovation Center for Climate Change, Jiangsu Province; Frontiers Science Center for Critical Earth Material Cycling, Nanjing University, Nanjing, China
5. Xin Huang (xinhuang@nju.edu.cn); School of Atmospheric Sciences, Nanjing University; Collaborative Innovation Center for Climate Change, Jiangsu Province; Frontiers Science Center for Critical Earth Material Cycling, Nanjing University, Nanjing, China
6. Aijun Ding (dingaj@nju.edu.cn); School of Atmospheric Sciences, Nanjing University; Collaborative Innovation Center for Climate Change, Jiangsu Province; Frontiers Science Center for Critical Earth Material Cycling, Nanjing University, Nanjing, China

STATEMET:

The paper is a non-peer reviewed preprint submitted to EarthArXiv. We have not yet submitted this paper to any journal.

Exacerbated ozone pollution in the greening northern China

Jiawei Xu[1,2,#], Sijia Lou[1,2,3#], Nan Wang[1,2], Lian Xue[1,2,3], Xin Huang[1,2,3], Aijun Ding[1,2,3*]

[1] School of Atmospheric Sciences, Nanjing University, Nanjing, 210023, China

[2]Collaborative Innovation Center of Climate Change, Jiangsu Province, Nanjing, 210023, China

[3]Frontiers Science Center for Critical Earth Material Cycling, Nanjing University, Nanjing, 210023, China

Correspondence: Aijun Ding (dingaj@nju.edu.cn)

Key words: ozone, afforestation projects, climate warming, air pollution in cities

SUMMARY

Biogenic volatile organic compounds are vital precursors of tropospheric ozone (O_3). In the past decades, northern China has witnessed the strongest enhancement of vegetation covers due to national afforestation projects; however, response of the vegetation greenness to near-surface O_3 remains unclear. By integrating measurements and numerical simulations, here we show that O_3 pollution in northern China has been enhanced by the unwind greening over the past two decades and will be exacerbated further in this century as the climate warming. We found that isoprene emission increased by 30% over northwestern China because of the vegetation increase and regional warming. Together with changes in anthropogenic emissions, it caused more O_3 pollution in city clusters in northern China. In the context of carbon peaking and carbon neutrality policy, vegetation greening will cause aggravating O_3 pollution by the middle of this century, which need to be considered in future air quality measures in China.

INTRODUCTION

Vegetation greenness has been increasing globally in past decades, partly due to the global warming and carbon dioxide (CO_2) fertilization[1-4]. At regional scale, extensive reforestation and afforestation has been conducted to address the challenge of climate change in terms of carbon capture and eroded [5-7]. Therefore, the greening rate shows strong regional diversity, with the most pronounced greening over intensively farmed or afforested areas, particularly in the Eurasia continent[8].

The northwestern China has witnessed the most intensive afforestation activities and featured the largest, around 2 million ha per year, afforested area in the world[9]. Such a fast vegetation greening is predominantly attributed to a series of large-scale afforestation program implemented by the Chinese government for the purpose of alleviating land degradation[10]. Noteworthily, the Three Northern Shelter Forest (TNSF) project, known as “the Green Great Wall”, increased the vegetation cover of the Gobi Desert from 5.05% to 13.2% from 1977 to 2016. Similarly, the Grain for Green project doubled the vegetation of the Loess Plateau since 1999[11-13]. Such a change of land use and land cover has been found a strong impact to regional climate in these region [13-16].

Vegetation greenness not only feedbacks to the local and regional climate, but also would greatly reshape the atmospheric chemistry via biological processes[1,17,18]. The biogenic volatile organic compounds (BVOCs), including

isoprene and terpenes, from terrestrial vegetation play an important role in atmospheric oxidative balance and the lifetimes of trace gases[19,20]. Due to the strong chemical reactivity, BVOCs, once released, would react with ambient oxidants such as the hydroxyl radical (OH) and subsequently contribute to ozone (O_3) and other oxidization products[21]. Vegetation emission has been found to greatly deteriorate O_3 pollution by supplying sufficient precursors for photochemical reactions, particularly when it mixed with anthropogenic pollutants like nitrogen oxides (NO_X)[22-25].

Ozone pollution is currently one of the key environmental challenges in China despite widely-implemented emission control measures[26,27]. In northern China, a hotspot with intensive anthropogenic emission, what role vegetation greenness has played in O_3 pollution during past decades remains unclear[28]. Most notably, Chinese government has launched a long-term plan of to increase forest cover to 26% by 2050[29]. How the future aggressive afforestation in a warming climate will influence regional O_3 pollution is unknown. In this study, by integrating satellite retrievals, in-situ observations, and climate-chemistry coupled modelling as well as future climate projections, we provide a quantitative understanding on the role of vegetation greening in atmospheric chemistry and O_3 pollution in the fast-greening northern China in the past decades and future.

RESULTS

Vegetation greening and ozone increase in northern China

Since the 1980s, multiple ecological afforestation projects have been carried out to prevent environmental deterioration in the semi-arid regions of northern China[8, 30]. Affected by these projects, notable growth of vegetation greening occurred in the Loess plateau, where the summertime leaf area index (LAI) and the Normalized Difference Vegetation Index (NDVI)[31, 32] increased by almost 77% and 46%, respectively, from 2001 to 2019 (Figure. 1a; Figure. S1). Under such a fast greenness expansion, it is expected that emission of BVOCs and O_3 concentration would consequently increase in the Loess plateau, especially in warm seasons (Figure. S2a). Indeed, ground-based observations from air quality monitoring network in China[33] show that near-surface O_3 concentration in northern China rises throughout the year with highest trend in summer (Figure. S2b). Over the fast-greening Loess Plateau and its downwind areas, near-surface O_3 concentrations increased by 8–24 ppb from 2013 to 2019 (Figure. 1b). The regional-scale O_3 enhancement cannot be explained alone by the change in anthropogenic emission[34], as which tends to cause different responses in urban and remote areas[35]. Emission estimation suggests a 23.6% reduction in NO_x emission together with a tiny change in anthropogenic volatile organic compounds (VOCs) emission, which cannot explain the strong

O_3 change in the Loess Plateau, a NO_x-limited area[36] (Figures. S3 and S4a). In addition, tropospheric ozone derived from the Ozone Monitoring Instrument (OMI)[37] increase continuous by 0.3 DU a^{-1} in northern China from 2005 to 2019, indicating drivers other than reduction of anthropogenic emissions, as the later only decreased since 2013.

Enhanced interaction of anthropogenic and biogenic sources

To explore the underlying mechanism of the soaring near-surface ozone over a greening northern China, we conducted meteorology-chemistry coupled model simulations for the past two decades. Model predictions were evaluated using ambient data at 317 air quality monitoring stations. As shown in Figure. S4b, the model well reproduced the observed spatial and temporal variations of O_3 concentrations in northern China. To investigate whether the afforestation project contributes to the rising O_3 pollution, we examined the impact of increased BVOC emissions (mainly isoprene) on the maximum 8-hour-average 90-percentile (M8A90) O_3 concentrations in summer (Figure. 2a). The M8A90 O_3 continued to exceed the Chinese National Ambient Air Quality Standard of 82 ppb[26] in northern China, which is recommended by the Ministry of Ecology and Environment China to characterize the statistic potential severe damage to human health[33].

Changes in emissions and climate are the two main factors that drive the variations in surface O_3 concentrations[38]. For the entire period 2001–2019, the emission of BVOCs around the Loess Plateau is expected to increase by 30% related to the afforestation alone. However, simulations using fixed meteorology and anthropogenic emissions of 2010 together with increasing BVOCs (GREEN) resulted in only a 2% increase in local M8A90 O_3 concentrations in the fastest greening area (Figure. 2a). The relatively low trend could be explained by the NO_x-limited regime over the Loess Plateau (Figure. S4a). However, the M8A90 O_3 concentrations increase more rapidly in city clusters in the North China Plain, east to the Loess Plateau (Figure. 2a).

It is known that isoprene can be oxidized within a few hours, while the oxidation products of isoprene, e.g. ISPD (lumped methacrolein, methyl vinyl ketone, methyl glyoxal, etc) and formaldehyde (HCHO)[39], have a much longer lifetime than isoprene itself, which can be transported thousands of kilometers away downwind from the biogenic source area (Figure. 2b). The satellite-measured HCHO to nitrogen dioxide (NO_2) ratios show a shift from a NO_x-limited regime for O_3 production in rural areas in the west to a VOCs-limited regime in the city clusters in the east (Figure. 2c). Therefore, those transported biogenic oxidized products, including HCHO, methyl vinyl ketone, methacrolein, methyl glyoxal, enhancing O_3 production under VOCs-limited conditions, resulting in a maximum increase of 7 ppb and more than 5 O_3 pollution events in urban areas (Figure. 2b-c).

Because of the vital roles of meteorological parameters on ozone production, climate change also affects surface O_3 concentrations via its impact on precursor gases, chemical environment associated with O_3 production and loss, and transport fluxes[40–46]. China is warming by more than 0.5 °C per decade[47,48], which could enhance biogenic emissions[49]. To investigate the effects of climate-warming-related biogenic emissions other than circulation changes, we conducted a simulation with the fixed meteorological fields in the year 2010 and varied BVOC emissions following the real climate change between two different periods, 2001–2003 and 2017–2019 (GREEN_CLI_EMIS). Isoprene emissions around the northern China are projected to increase by 174 Gg during the two decades. While the significant vegetation greenness between 2001 and 2019 contributed 80% to the total increment of BVOC emissions, climate change contributed the remaining 20%. The oxidation products are then increased by around 40% in the Loess Plateau (Figure. 3a-b). Our results reveal that the rapid climate warming amplifies isoprene emissions, and therefore tripling the increased M8A90 O_3 concentrations in downwind city clusters from 2001 to 2019 (Figure. 3c).

We also estimate the overall impact of climate change on O_3 concentrations between the two periods (GREEN_CLI), including combined changes in biogenic emissions, atmospheric chemistry, and transport. Compared to changes in biogenic emissions, isoprene oxidation products are reduced by 39% due to the overall effects of climate change from 2001 to 2019.

Meanwhile, HCHO concentrations have increased in the Loess Plateau (Figure. 3b). These variations are consistent with satellite-based HCHO measurement (Figure. S4c)[50], suggesting the accelerated atmospheric oxidation by climate change and a fast oxidization of isoprene into HCHO in the vegetation greening areas. With transport over hundreds of kilometers, this increased HCHO is continuously consumed and produces O_3 on its way to downwind city clusters (Figure. 3b). In addition, once this increased HCHO are transported to city clusters, the enhanced atmospheric oxidizing capacity also amplifies the BVOC-related O_3 production.

The M8A90 O_3 concentrations are estimated to increase by 5 ppb in the Loess Plateau during 2001–2019 (Figure. 3c). However, only one third of the increase is associated with changes in biogenic emissions, including the combined effects of vegetation greenness and climate warming. Instead, climate-driven change in transport is a significant driver of O_3 variations in those vegetation greening areas, where O_3 chemistry is not sensitive to biogenic emissions. In contrast, the M8A90 O_3 concentrations are estimated to increase by 9.6 ppb in the downwind city clusters (Figure. 3c), more than 60% of which were contributed from the vegetation greening and climate-warming-related changes in biogenic emissions. Our results highlight that climate change over the past two decades has enhanced the impact of western afforestation on O_3 concentrations in eastern cities, with an increase of 10% pollution events in recent years (Figure. 3d).

Ozone response to greening in a warming climate

To understand the long-term impact of the greening in this region, we further use climate projections to conduct model simulations. The Representative Concentration Pathway (RCP) and the Shared Socioeconomic Pathway-Representative Concentration Pathway (SSP) offer a broad range of future climate change and air pollution developments, considering challenges to various levels of mitigation and adaptation[51–53]. In this study, RCP8.5 is chosen as the reference scenario for climate change because it assumes a fragmented world that restricts international trade in energy and technology and describes an energy-intensive, fossil-based economy[54]. These assumptions are consistent with current global realities and fossil fuel production plans of major producing countries[55]. Furthermore, RCP8.5 represents the most severe future global warming scenario and is very close to SSP5-8.5 in CMIP6[56], which contains a significant climate change effect on vegetation greening.

As show in Figure 4a-b, when the global mean surface air temperature increases by 1.1 K from 2020 to 2050, the warming trend is more sensitive to the high latitudes in eastern China[56]. Therefore, the BVOC emissions from the Loess Plateau and northern China are expected to increase significantly over the next 30 years due to the afforestation projects and the ecosystem responses to climate change, respectively (Figure. 4a). In addition, the westerly

anomaly in 2050 will lead to more substantial transport of BVOCs and their oxidants from vegetation greening areas to downwind city clusters compared to 2020 (Figure. 4b).

Quantitative analyses from parallel simulations with different scenarios show that future changes in anthropogenic emissions will reduce the M8A90 O_3 concentrations in the Loess Plateau and city clusters by ~2-5% compared to 2020 (Figure. 4c; Figure. S5). In contrast, the effect of afforestation projects alone resulting a 3.3% increase M8A90 O_3 concentrations in eastern cities. Therefore, while stricter air quality control policies are expected to reduce O_3 pollution incidents in eastern urban agglomerations such as the North China Plain, these efforts are almost offset by the vegetation greening designed to protect from a warming climate.

Our results suggest that future climate warming will significantly amplify the impact of afforestation project on O_3 pollution in city clusters in the North China Plains. The overall effects of climate change and afforestation increase M8A90 O_3 concentrations by 8–22 ppb in the city clusters, much larger than the 2–6 ppb increase in the Loess Plateau from 2020 to 2050 (Figure. S6). Considering the unfavorable chemical environment for O_3 generation in 2050 compared to 2020 in eastern city clusters (e.g., an increase in relative humidity[57] and a decrease in solar radiation in eastern city clusters, Figure S7, Figure. 4c), a 3-fold increase in isoprene oxidation products such as HCHO in VOC-limited urban areas is the main reason for the increase in O_3 pollution (Figure. S8).

Compared to a previous study[58], our results magnify the O_3 pollution from climate-driven biogenic emissions by a factor of 2, indicating an essential contribution of vegetation greening to O_3 pollution in urban areas under a future warming climate. Previous study reported the O_3 pollution events increase by ~6% in eastern China from 2017 to 2050 due to changes in future anthropogenic emissions under SSP5-8.5 scenario[59]. In contrast, our results show that future changes in anthropogenic emissions will slightly increase the M8A90 O_3 concentrations in both the Loess Plateau and city clusters in 2050 under SSP5-8.5 scenario. Therefore, the afforestation projects under a warming climate may partly offset the air pollution control target, making it challenging to decrease O_3 pollution by reducing anthropogenic emissions.

DISCUSSION

In recent decades, with the most intensive afforestation activities and the largest afforested area in the world, O_3 pollution in northern China has also risen sharply. In this study, we integrate a regional chemistry model WRF-CMAQ and a biogenic emissions model (MEGAN) to access how the past and future O_3 concentrations might change with respect to the afforestation projects and climate change. From 2001 to 2019, the combined effects of vegetation greening and climate change increased the surface regional mean M8A90 O_3 concentrations over the Loess Plateau and eastern city clusters by 5 and 10

ppb over the Loess Plateau and eastern city clusters, respectively. Although changes in O_3 transport fluxes were the primary reason for O_3 variations in vegetation greening areas, more than 60% of M8A90 O_3 increments in eastern city clusters were associated with changes in biogenic emissions. Compared with 2001, isoprene emissions increased by 30% in 2019 around the vegetation greening areas, and its oxidation products. Under the future global warming scenario, the contribution of the western afforestation project to O_3 pollution events in the eastern city clusters is even larger. The overall effects of climate change and afforestation increase M8A90 O_3 concentrations by 8-22 ppb in eastern city clusters.

To achieve carbon neutrality goals, afforestation is expected worldwide. Although anthropogenic emissions are expected to decrease in the future, aiming to reduce O_3 exposure in cities, afforestation projects will partially offset the benefits of air pollution control. Moreover, our results imply that the afforestation project in remote areas under a warming climate may conflict with cities' air pollution control targets. In the future, stricter air quality control polices and afforestation projects of low isoprene emission tree species[60] are required to meet the both challenge of climate warming and O_3 pollution.

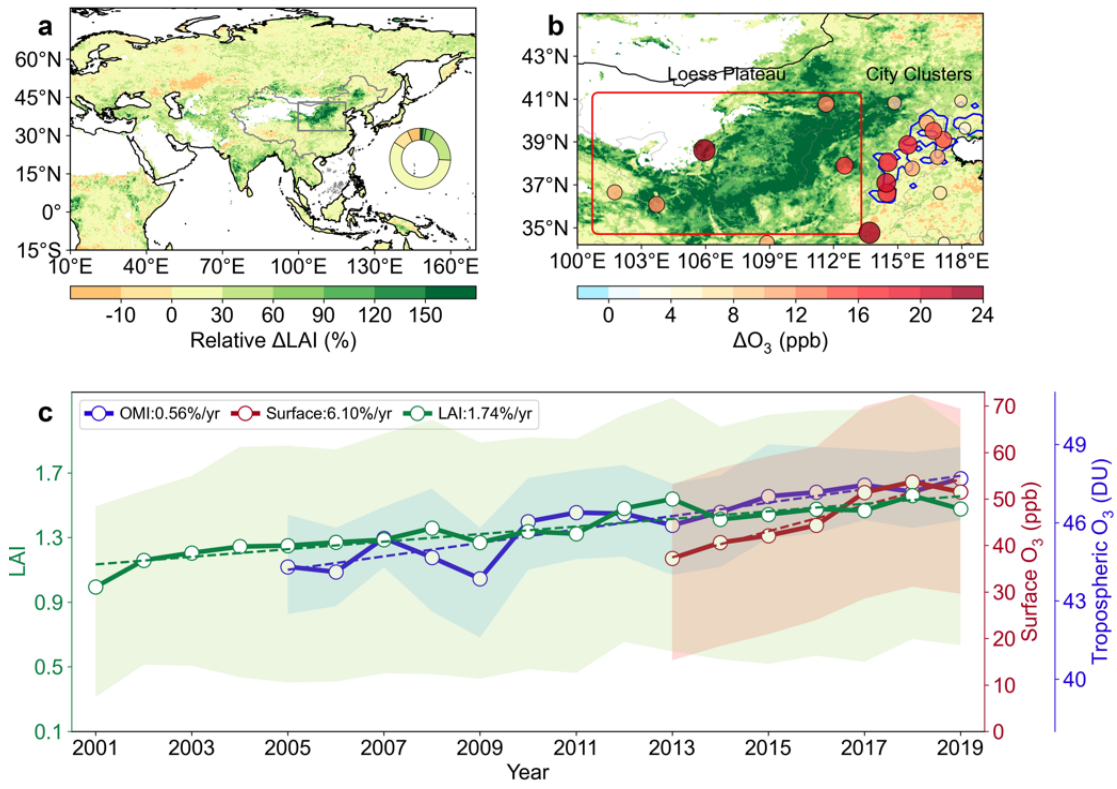

Figure 1. Changes of leaf area index (LAI) and ozone in Northern China. (a) LAI changes in summer between 2019 and 2001 (2019 minus 2001); pie chart shows the frequency of LAI changes in a; the grey rectangle shows regions in b. (b) Surface O_3 changes from 2013 to 2019 (2019 minus 2013, marked with filled circles), with the green background representing the LAI in a. Areas of the Loess Plateau and city clusters are indicated by red box and blue lines. (c) Regional mean concentrations (bold lines and circles) and their trends (thin lines) of summer LAI (green), tropospheric column ozone (blue) and surface ozone (red) over the Loess Plateau. Shadows show the 25th and 75th percentiles, respectively.

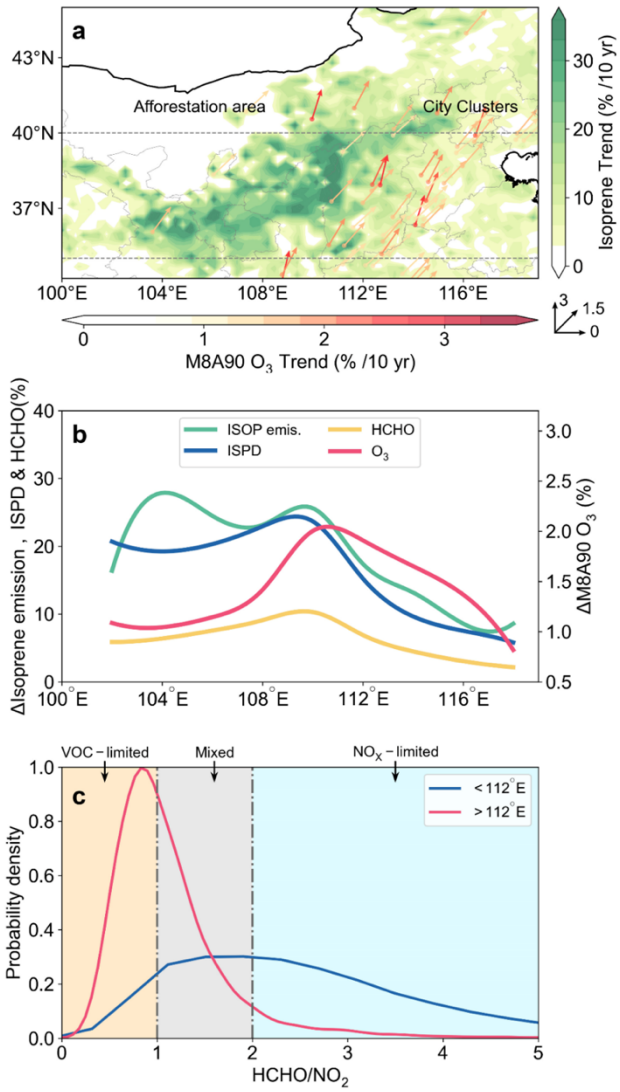

317

318 **Figure 2. Effect of afforestation on O_3 chemistry in northern China.**

319 (a) Simulation of isoprene emission (green contours) and M8A90 O_3 (red
320 arrows) trends from 2001 to 2019. Both directions and colors of the arrows
321 indicate the ozone change rates. Only M8A90 O_3 trends in high-NO_X-emission
322 areas are plotted (Areas with exceedance of 90th percentiles of summertime
323 NO_X emissions in this domain). (b) Meridional population-weighted mean (35–
324 41°N, area between dashed grey lines in a) changes of isoprene emission,
325 ISPD (lumped methacrolein, methyl vinyl ketone, methyl glyoxal, etc), HCHO
326 and M8A90 O_3 between the periods of 2001-2003 and 2017-2019 (2017-2019
327 minus 2001-2003). (c) Ratios of HCHO to NO_2 based on GOME-2 satellite data
328 in two regions. Note that meteorology and anthropogenic emissions were fixed
329 in 2010 while land cover/land change data was updated each year.

330

331

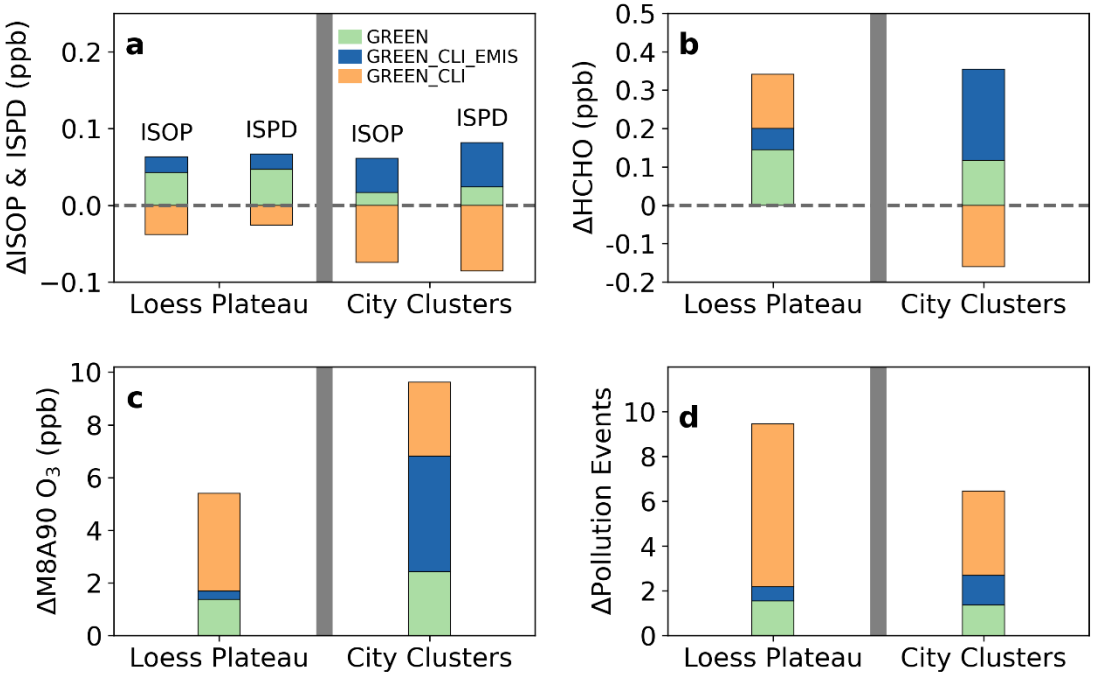

332

333

334 **Figure 3. Effect of climate change to emission and chemistry.**
335 Contribution of greening (green bar), climate change (enhanced-biogenic-
336 emission effect (blue bar) and accelerated-reaction-rates effect (orange bar))
337 to isoprene and ISPD (a), HCHO (b), M8A90 O_3 (c), and pollution events (d)
338 between 2001-2003 and 2017-2019 (2017-2019 minus 2001-2003). The
339 averaged areas are shown in Figure. 1b.

340

341

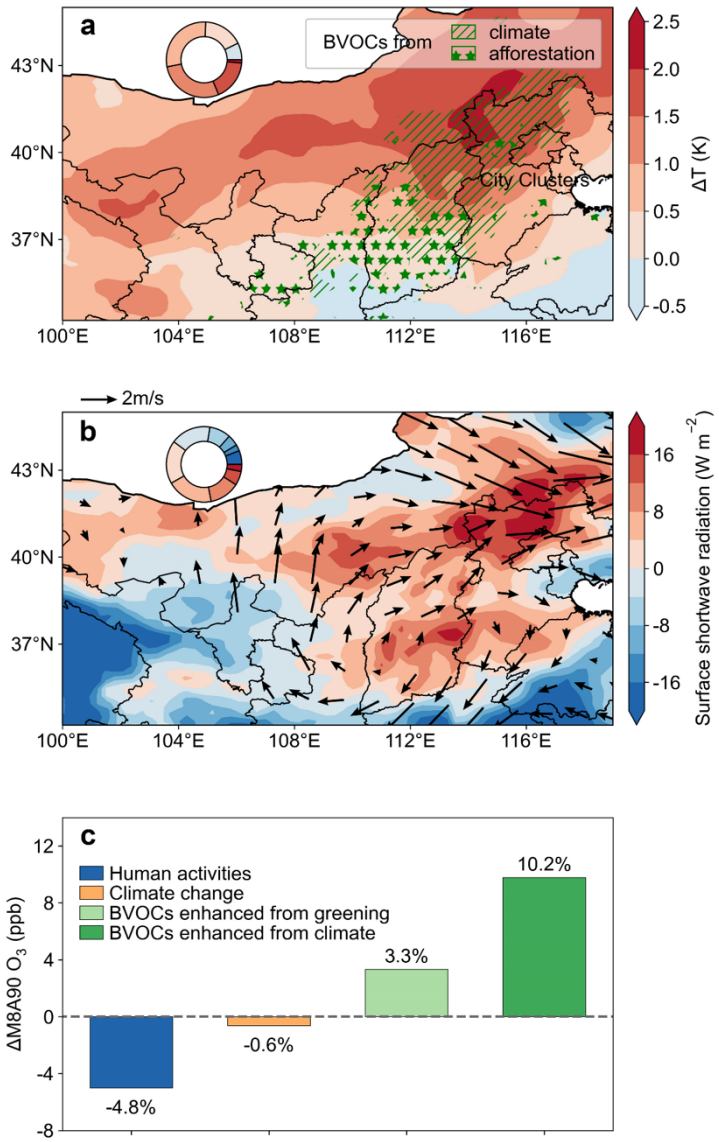

Figure 4. Impacts of climate change and vegetation greening on O_3 pollution in northern China. (a) Anomalous 2 m temperature during extreme pollution events between 2020 and 2050. The regions with an exceedance of 30% increment in isoprene emissions are illustrated by shadow. (b) Anomalous surface shortwave radiation and anomalous flows in 850hPa between 2020 and 2050. (c) Effects of human activities, climate and greenness to future O_3 in city clusters. Days with an exceedance of 90th percentiles across City Clusters in M8A90 O_3 are defined as extreme pollution events. Note: Pie charts in a and b represent the frequency of changes in temperature and shortwave radiation, respectively; all differences are calculated between two periods of 2049-2051 and 2019-2021 (2050-2020).

EXPERIMENTAL PROCEDURES

Resource availability

Lead contact

Further information and requests for resources and reagents should be directed to and will be fulfilled by the lead contact, Aijun Ding (dingaj@nju.edu.cn).

Materials availability

This study did not generate new unique materials.

Data and code availability

MODIS Satellite datasets are available from EARTHDATA (https://earthdata.nasa.gov/). NO_2 column datasets are available from OMI (https://www.temis.nl/index.php). O_3 column datasets are available from OMI (https://acd-ext.gsfc.nasa.gov/Data_services/cloud_slice/new_data.html). The CMIP5 RCP8.5 data are available from NCAR (https://rda.ucar.edu/datasets/ds316.1). The ozone data set used in this study can be downloaded from the website (https://doi.org/10.6084/m9.figshare.21158743.v1).

Observational and reanalysis data.

Summer ground-based observations of O_3, nitrogen dioxide (NO_2) and CO concentrations at more than 1400 stations since 2013 are obtained for model validation. The monitoring data are archived at the air monitoring data center of the Ministry of Ecology and Environment (MEE) of China. In 2013 MEE established the monitoring sites mainly in capital city of each province and then enlarged sites to most prefectural-level cities in China. Here, we evaluate modeling results with observational pollutants in northern China (Figure S4). Apart from surface observational data, column O_3 datasets from OMI are also used.

Regional chemical transport model.

Weather Research and Forecast – Community Multiscale Air Quality (WRF-CMAQ) modeling system was employed to investigate O_3 changes in northern China. This modelling system considers complex photochemical reactions and is wildly used to understand the impacts on air pollutants (especially for O_3) from meteorology and emission changes[61–64].

In this study, the model domain covered China and its surrounding area, centered at 39°N, 106.8°E with a horizontal grid resolution of 27 km, and 27 vertical layers from surface to 100 hPa. NCEP global final analysis (FNL) data were used as the initial and lateral boundary conditions of meteorological

variables with a 1°×1° spatial resolution that updates every 6 hours. While for modeling atmospheric chemistry, CMAQv5.1 was used and the major gas phase chemistry was represented by Carbon Bond version 05 (CB05) combined with Aerosol Module version 6 (AERO6). The initial and boundary conditions of chemical compositions came from a previous study (multi-year averaged FSDSMAM-hist using Community Earth System Model)[65] and, subsequently, dynamical downscaling to improve regional model simulations[66,67]. The key configuration of WRF-CMAQ included the Rapid Radioactive Transfer Model (RRTM) for longwave and shortwave radiation, the Noah Land Surface Model for land-atmospheric interactions, the Kain-Fritsch scheme for cumulus parameterization, the Lin microphysics scheme and the ACM2 boundary layer scheme. The anthropogenic emissions of China were obtained from Multi-resolution Emission Inventory for China (MEIC), which were developed by Tsinghua University and updated to 2017 levels [68].

Nine simulation scenarios were performed to investigate the effects of BVOC emissions (Supplementary Table S1).

(1) One BASE scenario was designed for model evaluation;

(2) Three HISTORY scenarios (GREEN, GREEN_CLI_EMIS and GREEN_CLI) were designed to estimate the impacts of afforestation projects and climate change on O_3 concentrations. For the GREEN scenario, only vegetation cover in MEGAN changed annually, leading to changes in BVOC emissions, while the meteorological parameters and anthropogenic emissions in CMAQ were fixed

in 2010. The GREEN_CLI_EMIS scenario was the same as GREEN, but meteorological parameters and land cover drive MEGAN vary yearly. The GREEN_CLI scenario was the same as GREEN_CLI_EMIS, but the meteorological parameters also vary yearly in CMAQ. Thus, the GREEN scenario represents the impact of afforestation projects on O_3 concentrations by changing BVOC emissions; the GREEN_CLI_EMIS scenario represents the impact of BVOC emissions (driven by climate change and afforestation projects) on O_3 concentrations; and the GREEN_CLI scenario examines the overall effects of climate change and afforestation projects on O_3 pollution.

(3) Five FUTURE scenarios have similar simulation designs to isolate the impacts of anthropogenic activities, afforestation projects, and climate change on future O_3 pollution. More specific details of our experimental designs can be found in supplemental information Experimental design.

Biogenic emissions.

The calculations of biogenic emissions in this study were performed using Model of Emissions of Gases and Aerosols from Nature version 2.1 (MEGANv2.1)[69]. It is widely used in simulation of BVOCs in China [22, 24, 50, 70]. MEGANv2.1 calculates emissions for 19 emission species include isoprene and monoterpenes based on following algorithm:

$$F_i=\gamma_i \sum \varepsilon_{i,j}\chi_j \quad (1)$$

where F_i, $\varepsilon_{i,j}$ and χ_j are emission amount, standard emission factor and fractional coverage of each plant functional type j of chemical species i. γ_i is emission activity factor, which is defined based on canopy environment coefficient, leaf area index (LAI), light (γ_L), temperature (γ_T), leaf age (γ_{LA}), soil moisture (γ_{SM}), and CO_2 inhibition (γ_{CI}):

$$\gamma_i = C_{CE} LAI \gamma_{L,i} \gamma_{T,i} \gamma_{LA,i} \gamma_{SM,i} \gamma_{CI,i} \quad (2)$$

Here, PFT data was from MODIS MCD12Q1 datasets and was classified from 8 vegetation types to 16 PFT types in MEGANv2.1 according to climatic criteria defined in previous study [71]. LAI data was also from MODIS datasets, with MODIS MOD15A2H for 2001 and MCD15A2H for 2002-2019, respectively. The PFT product is generated each year while the LAI products are composited every 8 days [31, 72]. At last, meteorological data was from WRF simulation.

Socioeconomic and climate scenarios

To quantify the relative impacts of future greening, climate change and anthropogenic emission change on O_3 concentrations, we vary these factors one at a time and compare the M8A90 O_3 attributable to each of these factors independently between 2020s and 2050s using the SSP-RCP scenarios.

In this paper, the future human activities scenarios are from SSP-RCPs of Coupled Model Intercomparison Project Phase 6 (CMIP6), which are combined with two dimensions[73]. One dimension is Shared Socioeconomic Pathways

(SSPs). The SSPs describe future changes in the energy mix, technological progress, population growth, diets, global collaboration, and so on. For example, SSP5 describes a high fossil-fueled development world[51, 74]. The other dimension is Representative Concentration Pathways (RCPs), which are the outcomes of climate policies. RCP8.5 assume paths limiting radiative forcing to 8.5 W m^{-2} in 2100. The CMIP5 RCP8.5 data are downloaded from NCAR[75].

In this study, the anthropogenic emissions (e.g., NO_x and VOCs emissions) are following SSP5-8.5 scenario[74]. Although cleaner combustion technologies and the shifting from coal use to liquefied petroleum gas (LPG) and electricity for energy, industry, and residential sectors substantially decrease ozone precursor gases emissions. Transportation, however, will primarily increase anthropogenic emissions in city clusters in 2050, associated with the growing economy and increasing car ownership in China [76,77]. The results start from 2015, and emissions are provided every 10 years during 2020 to 2100. Therefore, the NO_X and VOC emissions in different years are scaled up or down based on MEIC emission inventory in 2015.

ACKNOWLEDGMENTS

This work was supported by the National Natural Science Foundation of China (42293322), the Ministry of Science and Technology of the People's Republic of China (2022YFC3701105), and the Jiangsu Collaborative Innovation Center for Climate Change. We are grateful to the High-Performance Computing & Massive Data Center (HPC&MDC) of School of Atmospheric Science, Nanjing University for doing the numerical calculations in this paper on its Blade cluster system.

AUTHOR CONTRIBUTIONS

A.D. and X. H. designed the research. J.X. performed the simulations. J.X., S. L., X. H, and A. D. performed the overall analysis. J.X., and S. L. drafted the paper with the assistance from all authors.

COMPETING INTERESTS

The authors declare no competing interests.

REFERENCES

1. Piao, S., Wang, X., Park, T., Chen, C., Lian, X., He, Y., Bjerke, J.W., Chen, A., Ciais, P., Tømmervik, H., et al. (2020). Characteristics, drivers and feedbacks of global greening. Nat. Rev. Earth & Environment *1*, 14-27.https://doi.org/10.1038/s43017-019-0001-x.

2. Winkler, K., Fuchs, R., Rounsevell, M., and Herold, M. (2021). Global land use changes are four times greater than previously estimated. Nat. Commun. *12*, 2501.https://doi.org/10.1038/s41467-021-22702-2.
3. Macias-Fauria, M., Forbes, B.C., Zetterberg, P., and Kumpula, T. (2012). Eurasian Arctic greening reveals teleconnections and the potential for structurally novel ecosystems. Nature Clim. Change *2*, 613-618.https://doi.org/10.1038/nclimate1558.
4. Zhu, Z., Piao, S., Myneni, R.B., Huang, M., Zeng, Z., Canadell, J.G., Ciais, P., Sitch, S., Friedlingstein, P., Arneth, A., et al. (2016). Greening of the Earth and its drivers. Nature Clim. Change *6*, 791-795.https://doi.org/10.1038/nclimate3004.
5. Bastin, J.-F., Finegold, Y., Garcia, C., Mollicone, D., Rezende, M., Routh, D., Zohner Constantin, M., and Crowther Thomas, W. (2019). The global tree restoration potential. Science *365*, 76-79.https://doi.org/10.1126/science.aax0848.
6. Arora, V.K., and Montenegro, A. (2011). Small temperature benefits provided by realistic afforestation efforts. Nature Geosci. *4*, 514-518.https://doi.org/10.1038/ngeo1182.
7. Bright, R.M., Davin, E., O'Halloran, T., Pongratz, J., Zhao, K., and Cescatti, A. (2017). Local temperature response to land cover and management change driven by non-radiative processes. Nature Clim. Change *7*, 296-302.https://doi.org/10.1038/nclimate3250.
8. Chen, C., Park, T., Wang, X., Piao, S., Xu, B., Chaturvedi, R.K., Fuchs, R., Brovkin, V., Ciais, P., Fensholt, R., et al. (2019). China and India lead in greening of the world through land-use management. Nat. Sustain *2*, 122-129.https://doi.org/10.1038/s41893-019-0220-7.
9. Peng, S., Piao, S., Zeng, Z., Ciais, P., Zhou, L., Li Laurent, Z.X., Myneni Ranga, B., Yin, Y., and Zeng, H. (2014). Afforestation in China cools local land surface temperature. Proc. Natl. Acad. Sci. U.S.A. *111*, 2915-2919.https://doi.org/10.1073/pnas.1315126111.
10. Fang, J., Chen, A., Peng, C., Zhao, S., and Ci, L. (2001). Changes in Forest Biomass Carbon Storage in China Between 1949 and 1998. Science *292*, 2320-2322.https://doi.org/10.1126/science.1058629.
11. Chen, Y., Wang, K., Lin, Y., Shi, W., Song, Y., and He, X. (2015). Balancing green and grain trade. Nature Geosci. *8*, 739-741.https://doi.org/10.1038/ngeo2544.
12. Liu, J., Li, S., Ouyang, Z., Tam, C., and Chen, X. (2008). Ecological and socioeconomic effects of China's policies for ecosystem services. Proc. Natl. Acad. Sci. U.S.A. *105*, 9477.http://www.pnas.org/content/105/28/9477.abstract.
13. Xiao, J. (2014). Satellite evidence for significant biophysical consequences of the "Grain for Green" Program on the Loess Plateau in China. J. Geophys. Res. Biogeosci. *119*, 2261-2275.https://doi.org/10.1002/2014JG002820.
14. Tan, M., and Li, X. (2015). Does the Green Great Wall effectively decrease dust storm intensity in China? A study based on NOAA NDVI and weather station data. Land use policy *43*, 42-47.http://www.sciencedirect.com/science/article/pii/S0264837714002348.
15. Ge, J., Pitman, A.J., Guo, W., Zan, B., and Fu, C. (2020). Impact of revegetation of the Loess Plateau of China on the regional growing season water balance. Hydrol. Earth Syst. Sci. *24*, 515-533.https://hess.copernicus.org/articles/24/515/2020/.
16. Ge, J., Liu, Q., Zan, B., Lin, Z., Lu, S., Qiu, B., and Guo, W. (2022). Deforestation

intensifies daily temperature variability in the northern extratropics. Nat. Commun. *13*, 5955.https://doi.org/10.1038/s41467-022-33622-0.

17. Ma, M., Gao, Y., Wang, Y., Zhang, S., Leung, L.R., Liu, C., Wang, S., Zhao, B., Chang, X., Su, H., et al. (2019). Substantial ozone enhancement over the North China Plain from increased biogenic emissions due to heat waves and land cover in summer 2017. Atmospheric Chem. Phys. *19*, 12195-12207.https://acp.copernicus.org/articles/19/12195/2019/.
18. Yu, M., Zhou, W., Zhao, X., Liang, X., Wang, Y., and Tang, G. (2022). Is Urban Greening an Effective Solution to Enhance Environmental Comfort and Improve Air Quality? Environ. Sci. Technol.https://doi.org/10.1021/acs.est.1c07814.
19. Guenther, A., Hewitt, C.N., Erickson, D., Fall, R., Geron, C., Graedel, T., Harley, P., Klinger, L., Lerdau, M., McKay, W.A., et al. (1995). A global model of natural volatile organic compound emissions. J. Geophys. Res. Atmos. *100*, 8873-8892.https://doi.org/10.1029/94JD02950.
20. Di Carlo, P., Brune, W.H., Martinez, M., Harder, H., Lesher, R., Ren, X., Thornberry, T., Carroll, M.A., Young, V., Shepson, P.B., et al. (2004). Missing OH Reactivity in a Forest: Evidence for Unknown Reactive Biogenic VOCs. Science *304*, 722.http://science.sciencemag.org/content/304/5671/722.abstract.
21. Trainer, M., Williams, E.J., Parrish, D.D., Buhr, M.P., Allwine, E.J., Westberg, H.H., Fehsenfeld, F.C., and Liu, S.C. (1987). Models and observations of the impact of natural hydrocarbons on rural ozone. Nature *329*, 705-707.https://doi.org/10.1038/329705a0.
22. Situ, S., Guenther, A., Wang, X., Jiang, X., Turnipseed, A., Wu, Z., Bai, J., and Wang, X. (2013). Impacts of seasonal and regional variability in biogenic VOC emissions on surface ozone in the Pearl River delta region, China. Atmospheric Chem. Phys. *13*, 11803-11817.https://www.atmos-chem-phys.net/13/11803/2013/.
23. Xu, J., Huang, X., Wang, N., Li, Y., and Ding, A. (2021). Understanding ozone pollution in the Yangtze River Delta of eastern China from the perspective of diurnal cycles. Sci. Total Environ. *752*, 141928.http://www.sciencedirect.com/science/article/pii/S0048969720354577.
24. Liu, Y., Li, L., An, J., Huang, L., Yan, R., Huang, C., Wang, H., Wang, Q., Wang, M., and Zhang, W. (2018). Estimation of biogenic VOC emissions and its impact on ozone formation over the Yangtze River Delta region, China. Atmospheric Environ. *186*, 113-128.http://www.sciencedirect.com/science/article/pii/S1352231018303303.
25. Chen, W., Guenther, A.B., Shao, M., Yuan, B., Jia, S., Mao, J., Yan, F., Krishnan, P., and Wang, X. (2022). Assessment of background ozone concentrations in China and implications for using region-specific volatile organic compounds emission abatement to mitigate air pollution. Environmental Pollution *305*, 119254.https://www.sciencedirect.com/science/article/pii/S0269749122004687.
26. Li, K., Jacob, D.J., Liao, H., Shen, L., Zhang, Q., and Bates, K.H. (2018). Anthropogenic drivers of 2013–2017 trends in summer surface ozone in China. Proc. Natl. Acad. Sci. U.S.A. *116*, 422-427.https://www.pnas.org/content/pnas/early/2018/12/26/1812168116.full.pdf.
27. Lu, X., Hong, J., Zhang, L., Cooper, O.R., Schultz, M.G., Xu, X., Wang, T., Gao, M.,

Zhao, Y., and Zhang, Y. (2018). Severe Surface Ozone Pollution in China: A Global Perspective. Environ. Sci. Technol. Lett. *5*, 487-494.https://doi.org/10.1021/acs.estlett.8b00366.

28. Wang, T., Xue, L., Feng, Z., Dai, J., Zhang, Y., and Tan, Y. (2022). Ground-level ozone pollution in China: a synthesis of recent findings on influencing factors and impacts. Environmental Research Letters *17*, 063003.http://dx.doi.org/10.1088/1748-9326/ac69fe.
29. Wang, G., Innes, J.L., Lei, J., Dai, S., and Wu, S.W. (2007). China's Forestry Reforms. Science *318*, 1556.http://science.sciencemag.org/content/318/5856/1556.abstract.
30. Li, Y., Piao, S., Li Laurent, Z.X., Chen, A., Wang, X., Ciais, P., Huang, L., Lian, X., Peng, S., Zeng, Z., et al. (2018). Divergent hydrological response to large-scale afforestation and vegetation greening in China. Sci. Adv. *4*, eaar4182.https://doi.org/10.1126/sciadv.aar4182.
31. Yuan, H., Dai, Y., Xiao, Z., Ji, D., and Shangguan, W. (2011). Reprocessing the MODIS Leaf Area Index products for land surface and climate modelling. Remote Sens Environ *115*, 1171-1187.http://www.sciencedirect.com/science/article/pii/S0034425711000149.
32. Zheng, K., Wei, J.-Z., Pei, J.-Y., Cheng, H., Zhang, X.-L., Huang, F.-Q., Li, F.-M., and Ye, J.-S. (2019). Impacts of climate change and human activities on grassland vegetation variation in the Chinese Loess Plateau. Sci. Total Environ. *660*, 236-244.http://www.sciencedirect.com/science/article/pii/S0048969719300221.
33. Wang, Y., Gao, W., Wang, S., Song, T., Gong, Z., Ji, D., Wang, L., Liu, Z., Tang, G., Huo, Y., et al. (2020). Contrasting trends of $PM_{2.5}$ and surface-ozone concentrations in China from 2013 to 2017. Natl. Sci. Rev. *7*, 1331-1339.https://doi.org/10.1093/nsr/nwaa032.
34. Gaudel, A., Cooper, O.R., Chang, K.-L., Bourgeois, I., Ziemke, J.R., Strode, S.A., Oman, L.D., Sellitto, P., Nédélec, P., Blot, R., et al. (2020). Aircraft observations since the 1990s reveal increases of tropospheric ozone at multiple locations across the Northern Hemisphere. Sci. Adv. *6*, eaba8272.https://doi.org/10.1126/sciadv.aba8272.
35. Liu, Y., and Wang, T. (2020). Worsening urban ozone pollution in China from 2013 to 2017 – Part 2: The effects of emission changes and implications for multi-pollutant control. Atmospheric Chem. Phys. *20*, 6323-6337.https://acp.copernicus.org/articles/20/6323/2020/.
36. Sillman, S. (1995). The use of NO_y, H_2O_2 and HNO_3 as indicators for ozone-NO_x-hydrocarbon sensitivity in urban locations. J. Geophys. Res. Atmos. *100*, 14175-14188.http://dx.doi.org/10.1029/94JD02953.
37. Ziemke, J.R., Chandra, S., Duncan, B.N., Froidevaux, L., Bhartia, P.K., Levelt, P.F., and Waters, J.W. (2006). Tropospheric ozone determined from Aura OMI and MLS: Evaluation of measurements and comparison with the Global Modeling Initiative's Chemical Transport Model. J. Geophys. Res. Atmos. *111*.https://doi.org/10.1029/2006JD007089.
38. Sun, L., Xue, L., Wang, Y., Li, L., Lin, J., Ni, R., Yan, Y., Chen, L., Li, J., Zhang, Q., and Wang, W. (2019). Impacts of meteorology and emissions on summertime surface ozone increases over central eastern China between 2003 and 2015. Atmospheric Chem. Phys. *19*, 1455-1469.https://acp.copernicus.org/articles/19/1455/2019/.

39. Yarwood, G., Rao, S., Yocke, M., and Whitten, G. (2005). Updates to the carbon bond chemical mechanism: CB05 final report to the US EPA. 2005/12/08. http://www.camx.com/publ/pdfs/CB05_Final_Report_120805.pdf.
40. Sanderson, M.G., Jones, C.D., Collins, W.J., Johnson, C.E., and Derwent, R.G. (2003). Effect of Climate Change on Isoprene Emissions and Surface Ozone Levels. Geophys. Res. Lett. *30*.https://doi.org/10.1029/2003GL017642.
41. Ebi Kristie, L., and McGregor, G. (2008). Climate Change, Tropospheric Ozone and Particulate Matter, and Health Impacts. Environ. Health Perspect. *116*, 1449-1455.https://doi.org/10.1289/ehp.11463.
42. Jacob, D.J., and Winner, D.A. (2009). Effect of climate change on air quality. Atmospheric Environ. *43*, 51-63.https://www.sciencedirect.com/science/article/pii/S1352231008008571.
43. Fu, T.-M., Zheng, Y., Paulot, F., Mao, J., and Yantosca, R.M. (2015). Positive but variable sensitivity of August surface ozone to large-scale warming in the southeast United States. Nature Clim. Change *5*, 454-458.https://doi.org/10.1038/nclimate2567.
44. Kramshøj, M., Vedel-Petersen, I., Schollert, M., Rinnan, Å., Nymand, J., Ro-Poulsen, H., and Rinnan, R. (2016). Large increases in Arctic biogenic volatile emissions are a direct effect of warming. Nature Geosci. *9*, 349-352.https://doi.org/10.1038/ngeo2692.
45. Zhang, Y., and Wang, Y. (2016). Climate-driven ground-level ozone extreme in the fall over the Southeast United States. Proc. Natl. Acad. Sci. U.S.A. *113*, 10025-10030.https://doi.org/10.1073/pnas.1602563113.
46. Zhang, Y., Cooper, O.R., Gaudel, A., Thompson, A.M., Nédélec, P., Ogino, S.-Y., and West, J.J. (2016). Tropospheric ozone change from 1980 to 2010 dominated by equatorward redistribution of emissions. Nature Geosci. *9*, 875-879.https://doi.org/10.1038/ngeo2827.
47. NOAA National Centers for Environmental Information (2020). State of the Climate: Monthly Global Climate Report for Annual 2020. https://www.ncei.noaa.gov/access/monitoring/monthly-report/global/202013.
48. Song, F., Zhang Guang, J., Ramanathan, V., and Leung, L.R. (2022). Trends in surface equivalent potential temperature: A more comprehensive metric for global warming and weather extremes. Proc. Natl. Acad. Sci. U.S.A. *119*, e2117832119.https://doi.org/10.1073/pnas.2117832119.
49. Stavrakou, T., Müller, J.F., Bauwens, M., De Smedt, I., Van Roozendael, M., Guenther, A., Wild, M., and Xia, X. (2014). Isoprene emissions over Asia 1979-2012: impact of climate and land-use changes. Atmospheric Chem. Phys. *14*, 4587-4605.https://acp.copernicus.org/articles/14/4587/2014/.
50. Wang, H., Wu, Q., Guenther, A.B., Yang, X., Wang, L., Xiao, T., Li, J., Feng, J., Xu, Q., and Cheng, H. (2021). A long-term estimation of biogenic volatile organic compound (BVOC) emission in China from 2001–2016: the roles of land cover change and climate variability. Atmospheric Chem. Phys. *21*, 4825-4848.https://acp.copernicus.org/articles/21/4825/2021/.
51. O'Neill, B.C., Tebaldi, C., van Vuuren, D.P., Eyring, V., Friedlingstein, P., Hurtt, G., Knutti, R., Kriegler, E., Lamarque, J.F., Lowe, J., et al. (2016). The Scenario Model Intercomparison Project (ScenarioMIP) for CMIP6. Geosci. Model Dev. *9*, 3461-

3482.https://gmd.copernicus.org/articles/9/3461/2016/.

52. IPCC (2021). Climate Change 2021: The Physical Science Basis. Contribution of Working Group I to the Sixth Assessment Report of the Intergovernmental Panel on Climate Change.

53. van Vuuren, D.P., Edmonds, J., Kainuma, M., Riahi, K., Thomson, A., Hibbard, K., Hurtt, G.C., Kram, T., Krey, V., Lamarque, J.-F., et al. (2011). The representative concentration pathways: an overview. Clim Change *109*, 5.https://doi.org/10.1007/s10584-011-0148-z.

54. Riahi, K., Rao, S., Krey, V., Cho, C., Chirkov, V., Fischer, G., Kindermann, G., Nakicenovic, N., and Rafaj, P. (2011). RCP 8.5—A scenario of comparatively high greenhouse gas emissions. Clim Change *109*, 33.https://doi.org/10.1007/s10584-011-0149-y.

55. SEI, I., ODI, E3G, and UNEP. 2021 Production Gap Report. https://productiongap.org/2021report/.

56. Zhu, H., Jiang, Z., and Li, L. (2021). Projection of climate extremes in China, an incremental exercise from CMIP5 to CMIP6. Sci. Bull. *66*, 2528-2537.https://www.sciencedirect.com/science/article/pii/S2095927321005077.

57. Lei, Y., Yue, X., Liao, H., Zhang, L., Zhou, H., Tian, C., Gong, C., Ma, Y., Cao, Y., Seco, R., et al. (2022). Global Perspective of Drought Impacts on Ozone Pollution Episodes. Environ. Sci. Technol. *56*, 3932-3940.https://doi.org/10.1021/acs.est.1c07260.

58. Liu, S., Xing, J., Zhang, H., Ding, D., Zhang, F., Zhao, B., Sahu, S.K., and Wang, S. (2019). Climate-driven trends of biogenic volatile organic compound emissions and their impacts on summertime ozone and secondary organic aerosol in China in the 2050s. Atmospheric Environ. *218*, 117020.https://www.sciencedirect.com/science/article/pii/S1352231019306594.

59. Zeng, X., Gao, Y., Wang, Y., Ma, M., Zhang, J., and Sheng, L. (2022). Characterizing the distinct modulation of future emissions on summer ozone concentrations between urban and rural areas over China. Sci. Total Environ. *820*, 153324.https://www.sciencedirect.com/science/article/pii/S0048969722004168.

60. Sharkey, T.D., Wiberley, A.E., and Donohue, A.R. (2008). Isoprene Emission from Plants: Why and How. Ann. Bot *101*, 5-18.https://doi.org/10.1093/aob/mcm240.

61. Gilliland, A.B., Hogrefe, C., Pinder, R.W., Godowitch, J.M., Foley, K.L., and Rao, S.T. (2008). Dynamic evaluation of regional air quality models: Assessing changes in O_3 stemming from changes in emissions and meteorology. Atmospheric Environ. *42*, 5110-5123.http://www.sciencedirect.com/science/article/pii/S1352231008001374.

62. Wang, N., Lyu, X., Deng, X., Huang, X., Jiang, F., and Ding, A. (2019). Aggravating O_3 pollution due to NO_x emission control in eastern China. Sci. Total Environ. *677*, 732-744.http://www.sciencedirect.com/science/article/pii/S0048969719319333.

63. Zheng, B., Zhang, Q., Zhang, Y., He, K.B., Wang, K., Zheng, G.J., Duan, F.K., Ma, Y.L., and Kimoto, T. (2015). Heterogeneous chemistry: a mechanism missing in current models to explain secondary inorganic aerosol formation during the January 2013 haze episode in North China. Atmospheric Chem. Phys. *15*, 2031-2049.https://acp.copernicus.org/articles/15/2031/2015/.

64. Wang, N., Guo, H., Jiang, F., Ling, Z.H., and Wang, T. (2015). Simulation of ozone

formation at different elevations in mountainous area of Hong Kong using WRF-CMAQ model. Sci. Total Environ. *505*, 939-951.http://www.sciencedirect.com/science/article/pii/S0048969714015150.

65. Xue, L., Ding, A., Cooper, O., Huang, X., Wang, W., Zhou, D., Wu, Z., McClure-Begley, A., Petropavlovskikh, I., Andreae, M.O., and Fu, C. (2020). ENSO and Southeast Asian biomass burning modulate subtropical trans-Pacific ozone transport. Natl. Sci. Rev. *8*.https://doi.org/10.1093/nsr/nwaa132.
66. Gao, Y., Fu, J.S., Drake, J.B., Lamarque, J.F., and Liu, Y. (2013). The impact of emission and climate change on ozone in the United States under representative concentration pathways (RCPs). Atmospheric Chem. Phys. *13*, 9607-9621.https://acp.copernicus.org/articles/13/9607/2013/.
67. Caldwell, P., Chin, H.-N.S., Bader, D.C., and Bala, G. (2009). Evaluation of a WRF dynamical downscaling simulation over California. Clim Change *95*, 499-521.https://doi.org/10.1007/s10584-009-9583-5.
68. Li, M., Zhang, Q., Zheng, B., Tong, D., Lei, Y., Liu, F., Hong, C., Kang, S., Yan, L., Zhang, Y., et al. (2019). Persistent growth of anthropogenic non-methane volatile organic compound (NMVOC) emissions in China during 1990–2017: drivers, speciation and ozone formation potential. Atmos. Chem. Phys. *19*, 8897-8913.https://acp.copernicus.org/articles/19/8897/2019/.
69. Guenther, A.B., Jiang, X., Heald, C.L., Sakulyanontvittaya, T., Duhl, T., Emmons, L.K., and Wang, X. (2012). The Model of Emissions of Gases and Aerosols from Nature version 2.1 (MEGAN2.1): an extended and updated framework for modeling biogenic emissions. Geosci. Model Dev. *5*, 1471-1492.https://www.geosci-model-dev.net/5/1471/2012/.
70. Tie, X., Geng, F., Peng, L., Gao, W., and Zhao, C. (2009). Measurement and modeling of O_3 variability in Shanghai, China: Application of the WRF-Chem model. Atmospheric Environ. *43*, 4289-4302.https://doi.org/10.1016/j.atmosenv.2009.06.008.
71. Bonan, G.B., Levis, S., Kergoat, L., and Oleson, K.W. (2002). Landscapes as patches of plant functional types: An integrating concept for climate and ecosystem models. Global Biogeochem Cycles *16*, 5-1-5-23.https://doi.org/10.1029/2000GB001360.
72. Friedl, M.A., Sulla-Menashe, D., Tan, B., Schneider, A., Ramankutty, N., Sibley, A., and Huang, X. (2010). MODIS Collection 5 global land cover: Algorithm refinements and characterization of new datasets. Remote Sens Environ *114*, 168-182.http://www.sciencedirect.com/science/article/pii/S0034425709002673.
73. Gidden, M.J., Riahi, K., Smith, S.J., Fujimori, S., Luderer, G., Kriegler, E., van Vuuren, D.P., van den Berg, M., Feng, L., Klein, D., et al. (2019). Global emissions pathways under different socioeconomic scenarios for use in CMIP6: a dataset of harmonized emissions trajectories through the end of the century. Geosci. Model Dev. *12*, 1443-1475.https://gmd.copernicus.org/articles/12/1443/2019/.
74. Kriegler, E., Bauer, N., Popp, A., Humpenöder, F., Leimbach, M., Strefler, J., Baumstark, L., Bodirsky, B.L., Hilaire, J., Klein, D., et al. (2017). Fossil-fueled development (SSP5): An energy and resource intensive scenario for the 21st century. Glob Environ Change *42*, 297-315.https://www.sciencedirect.com/science/article/pii/S0959378016300711.
75. Monaghan, A.J., Steinhoff, D.F., Bruyere, C.L., and Yates, D. (2014). NCAR CESM

Global Bias-Corrected CMIP5 Output to Support WRF/MPAS Research. Research Data Archive at the National Center for Atmospheric Research, Computational and Information Systems Laboratory.

76. Rao, S., Klimont, Z., Smith, S.J., Van Dingenen, R., Dentener, F., Bouwman, L., Riahi, K., Amann, M., Bodirsky, B.L., van Vuuren, D.P., et al. (2017). Future air pollution in the Shared Socio-economic Pathways. Glob Environ Change *42*, 346-358.https://www.sciencedirect.com/science/article/pii/S0959378016300723.

77. Zhang, R., and Hanaoka, T. (2022). Cross-cutting scenarios and strategies for designing decarbonization pathways in the transport sector toward carbon neutrality. Nat. Commun. *13*, 3629.https://doi.org/10.1038/s41467-022-31354-9.